Quantitative Evaluation of Standing Stabilization Using Stiff and Compliant Actuators

Author Names Omitted for Anonymous Review. Paper-ID [add your ID here]

***Abstract*—In this paper we evaluate the benefits of series elastic actuation in performing a balancing task on a humanoid robot. By replacing an elastic transmission with a rigid one it was possible to repeat the very same experiment in two different conditions: (1) on a humanoid robot with series elastic actuators (SEA) at the ankle and at the knee; (2) on the same humanoid robot with the series elastic elements replaced by rigid transmissions. The proposed experiments consist in perturbing a balanced posture with an impulsive force, $100ms$ in duration. Perturbations were applied in two different scenarios: either by hitting the robot on the upper body ($450N$ in amplitude), or by hitting the robot support platform ($900N$ in amplitude). Experimental conditions were controlled in several ways. On one hand, the applied perturbations were controlled to be repeatable by performing the experiments several times, averaging over trials and plotting the standard deviation of all measured quantities. On the other hand, the static behavior of the balancing controller was controlled to be the same across all conditions. In particular, the static stiffness of the rigid and elastic actuators were tuned to be equal. In practice, by observing that the overall actuator stiffness is the sum of the active stiffness (the proportional component of the controller) and the transmission stiffness, the active stiffness component was increased with SEAs so as to maintain the overall static stiffness comparable to the one with rigid actuators. The balance controller (to keep the zero moment point within the support polygon) was instead kept constant across the all trials. With this assumption, static responses were the same in the two conditions; differences appeared only during the dynamic response and were motivated by different proportions between active and passive stiffness. In both the considered scenarios, results show that series elasticity simplifies the role of the balancing controller by low pass filtering the dynamics of the zero moment point. This results in faster balance recover with SEAs which was observed in all experimental conditions.**

I. Introduction

Humanoid robots are designed to have anthropomorphic structure with body, arms, and legs. While the bipedal walking solves the mobility issue to allow humanoids to ambulate, it is also interesting to understand how the leg could help the operation of arms. During the execution of manipulation tasks of the upper limbs, the balancing capability becomes essential in order to stabilize the robots themselves. Stability and soft interactions are commonly the desired safety feature for the co-existence of robots and humans, which provides the viability of stable manipulation during standing for humanoids.

To balance the robot in a standing posture, introducing the compliance with passivity is one of the effective approaches. The compliance provides the soft interaction during the contacts to prevent large collision forces, and it also naturally raises up the force and torque to recover to the equilibrium as deformation accumulates. The passivity property is commonly introduced to guarantee the stability because it attenuates the excessive energy interchange during the unavoidable collisions while the robot is interacting with the environment. For the robots with torque controlled joints, such as the Sarcos robot [1] [2] and the DLR robots [3] [4], this is realized by controlling the virtual compliance, namely the virtual spring and dampers, at the center of mass (COM) followed by computing the desired joint torques in order to generate forces at contacts to achieve such virtual spring and damper effect.

Fig. 1. A picture of the robot used in the experiments with a zoom on the series elastic element which was replaced with a rigid element during experiments with the rigid transmission.

However, considering the torque controlled actuators are less technically available, it is also interesting to investigate the implementation of the compliant behavior using position controlled actuators. The work in [5] presents the formula to modulate positional references of the COM of the robot based on the center of pressure (COP) feedback in feet. The control framework was applied to both the stiff actuated joints and the series elastic ones. It was found that by trading off the control bandwidth using the elastic springs between the gearbox's shaft and the output link, the system in return gains the benefits of instantaneous shock absorption since the controlled compliance merely using stiff actuators has an inevitable delay.

Most humanoid platforms developed in the past focuses on the mobility issue. The Honda ASIMO[6], HUBO [7], and HRP4-C[8] were developed for bipedal walking. The Sony QRIO [9] and the Aldebaran NAO [10] were the small scale humanoids for the purposes of entertainment, research and education. On the hardware level of these above-mentioned humanoids, the actuation has the stiff position controlled joints in common. It provides precise position tracking yet the adaptability to physical interaction or the robustness to accidental collisions are limited.

Although the collision issue in the real world application of the humanoids can be partly addressed by actively controlling the compliance, there is still the necessity of safety enhancement at the hardware level. Incorporating compliant material into the actuation system, such as the series elastic actuators (SEA) [11], can be useful. Unlike the compliance produced by the controller, the physical compliance can tackle impacts within short time instant, which is similar to the spring suspension system for cars. This concern motivates the development of humanoid robots comprising SEAs. The first robot used SEA was the Cog robot developed by Brooks et al. [12]. Later, there are the following development of the M2V2 robot by Pratt and Krupp [13], and the DOMO upper body by Edsinger and Weber [14] which constituted the robots from Meka Robotics. Also, the similar design is employed for the BioRob arm[15]. The compact size SEA developed by Tsagarakis et al. [16] was integrated into the COMAN humanoid [17]. The DLR hand arm system [18] exploits the floating spring joints (FSJ) [19].

The experimental testbed in this paper is the upgraded iCub2 platform which is inspired by features of the COMAN humanoid [16]. In this upgraded version, the knee and ankle joints are equipped by the SEAs with high resolution position sensing for accurate torque measurement. Moreover, the SEA unit also provides the possibility to lock the elastic mechanism to make a complete stiff joint. In this paper, the stabilization control based on the principle in [5] is applied on this platform for balancing in an upright standing posture. A comparison study is hereby investigated to quantitatively delineate the different characteristics between the stiff and the SEA joints. A collision test is designed using falling mass to examine the performance.

This paper is organized as follows. Section II describes the mechanical design and the specifications of the SEA units. Section III presents the experimental set-up, data and the analysis. The conclusion and future work are made in Section IV.

II. Design of the SEA elastic module

The SEA module employed for the experiments presented in this paper was developed from a similar design sub-assembly of the COMAN robot. A suitable value for the torsional stiffness of the elastic module, for tasks such as walking and balancing, was determined with experiments with the COMAN humanoid robot. The optimal value was determined to be in the range from 300 to $350[Nm/rad]$. Being the maximum leg actuator torque in the ballpark of $40[Nm]$, the corresponding passive angular deflection of the SEA which permits the delivery of the peak torque within the elastic deflection range is in the order of of $0.1333[rad]$.

The elastic module of the COMAN robot however did not allow to obtain such torsional stiffness values. Walking experiments showed that the elastic deflection limit was reached at $\approx 50\%$ the maximum torque, therefore reducing the advantages of the integration of SEA modules. We therefore considered possible alternative designs of the elastic module.

The SEA module of COMAN comprises three pairs of opposing helical springs [16]. We firstly considered substituting the original springs with different helical springs, disk springs and volute springs while keeping the size of the elastic module as close as possible to the size of the original design as well as a different design comprising leaf springs.

However none of these alternatives allowed to obtain the desired torsional rigidity. Indeed the spring selection presents a very delicate trade-off problem between the spring stiffness, its maximum deflection before yielding (that required bigger springs) and the available space (that constrained the size of the springs).

We finally considered a "curved beam" spring that we dubbed "C-spring", because of its shape, somewhat similar to the Robonaut torsion spring [20].

A preliminary calculation of the deflection of a curved beam, was based on the classical equations of linear elasticity [21]. We employed Castigliano's theorem to derive a closed form analytical equation that relates the spring geometry to its torsional stiffness.

We then conducted a finite element analysis (FEA) on the "C-spring" to verify its torsional stiffness value: the displacement under load closely matched the analytical predictions and the maximum Von Mises equivalent stresses was confirmed to be well below the elastic limit of the material.

The interested reader is referred to [22] for additional details regarding the mechatronic design of the SEA module.

The proposed elastic element design has the advantage of providing great design flexibility if compared to other implementations based on helical springs. Indeed the dimensioning of the elastic element can be effectively performed to match a wide range of desired stiffness levels.

A. Elastic element embodiment

The final embodiment of the subsystem is represented in Fig.2. Two magnetic encoders (an absolute one and a high resolution realtive one) were integrated in the module for deriving joint torque information.

Fig.2(a) shows a cross section drawing of the elastic module. Fig.2(b) shows in detail how the module is assembled; the figure also shows the protrusions in the "Motor output" part that constitute the hardware limits for the spring.

We chose to construct the elastic element in X5CrNiCuNb16-4[1] stainless steel because of it's ultimate tensile strength (UTS) of $1100[MPa]$.

The shape we adopted for the elastic element also provides a very convenient way for changing the connecting element. If a rigid joint is required (as in the case of the present study) it is sufficient to replace the SEA spring with a rigid element as shown in Fig.3.

III. Standing Stabilization Control

Fig. 4(a) shows the simplified model where the robot is represented by an inverted pendulum connected with a foot by

[1] see material datasheet
http://www.aksteel.com/pdf/markets_products/stainless/precipitation/17-4_PH_Data_Sheet.pdf

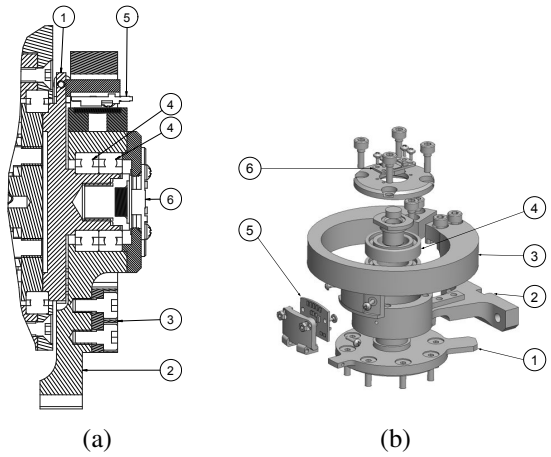

Fig. 2. SEA module. The figure shows a cross section drawing (a), and a CAD view (b) of the "C-spring" SEA module. The labelled sub-components are: the motor output part (1), the SEA module output part (2), the "C-spring" (3), the two ball bearings (4), the high resolution relative encoder based on the AS5311 IC (5), and the absolute magnetic encoder based on the AS5040 IC (6).

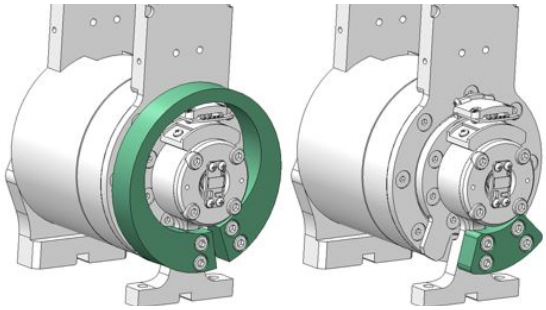

Fig. 3. Rigid joint substitution. The figure shows how by substituting the element connecting the motor output and the joint output is was possible to obtain a SEA joint (a) and a rigid joint (b) on the same setup.

a torsion spring with the stiffness k_s. Note that k_s represents the stiffness contributed by the mechanism at the COM level, which can be varied according to mechanical configuration (locking and unlocking the C spring). The parameter k is the resultant stiffness observed from the COM's behavior which is determined by both the mechanism and the active controller. In the case of the SEA joint, k_s can be small value compared to the structure stiffness, hereby we mark the real COM black and the referential COM red. Fig. 4(b) provides an intuitive scenario that the change of COM reference can control the resultant stiffness observed from external load. In this case, the forward perturbation causes the COP move forward, the robot would behave in a more compliant manner if the COM reference could be modulated forward accordingly. Contrarily, if the COM reference moves in the opposite direction as the COP, the observed stiffness k would be higher than the real stiffness k_s, which is not preferred for stabilization since more energy is injected into the system and thus causes instability.

To stabilize the standing posture, a compliance control scheme is applied based on the positional modification of

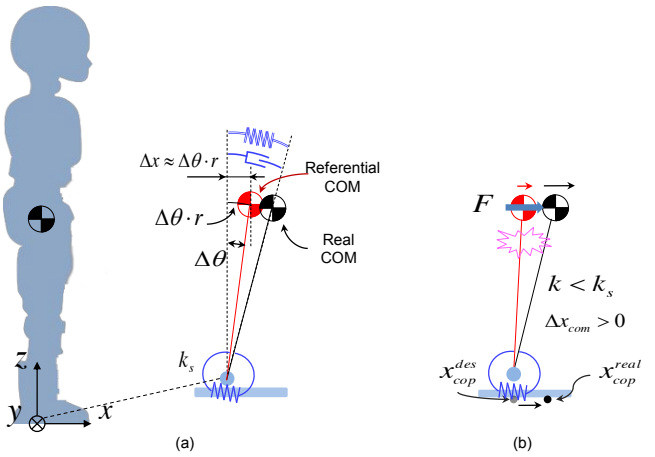

Fig. 4. Compliance control by regulating the COM reference

the COM using the COP feedback. This is analogous to the admittance control technique which the position perturbations computed from the applied forces are superimposed to the reference position of a stiff position controlled robot for emulating the compliant behavior.

Define θ^{des} and x_{cop}^{des} as the desired angular position of ankle and the COP at the static equilibrium respectively, $\Delta x_{cop} = x_{cop}^{real} - x_{cop}^{des}$ as the input of the controller and $\Delta\theta$ as output of the controller. The compliant control for the ankle joint is expressed in a simple PID form as

$$\Delta\theta(i) = k_p \Delta x_{cop}(i) - k_d \Delta\dot{x}_{cop}(i) - k_i \sum_{j=N}^{0} \Delta\tilde{x}_{cop}(i-j)\Delta t, \tag{1}$$

where $k_p > 0$, $k_d > 0$, and $k_i > 0$ are the proportional, derivative, and integral gains respectively, and Δt is the sampling time.

The proportional gain k_p determines how much the reference COM should be modified in the same direction as the COP in order to keep away from the collision. Hence, the bigger the k_p is, the more compliant the robot becomes. The gain k_d plays a role of the damping effect on the referenced COM motion. Considering the compliant behavior will bring the steady state error, the integral term is included for removing the static offset of COP. $\tilde{x}_{cop}$ denotes the filtered COP signal for the integral term. The integral windup is solved by using a limited time window with N samples in addition to the setting of upper and lower limits.

IV. Experiments and Comparison

In this section the balancing performance of the robot is evaluated through two different balancing experiments: an direct impact on the robots body and an impact on a mobile platform on which the robots stands. Each of the two experiments is performed first with the robot ankles equipped with the elastic elements and then connected through the stiff connection. It must be noticed that the employment of the elastic elements increases the overall compliance of the

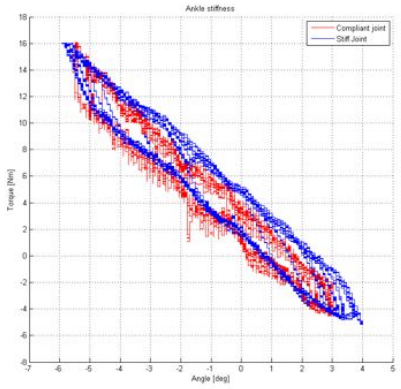

Fig. 5. The overall (active+passive) stiffness at the ankle joint. The gains of the balancing controller were experimentally tuned in order to achieve the same equivalent stiffness both with stiff and series elastic joints (stiff joint: Kp = 0.4, Kd=0.005; elastic joint: Kp=0.3, Kd=0.08).

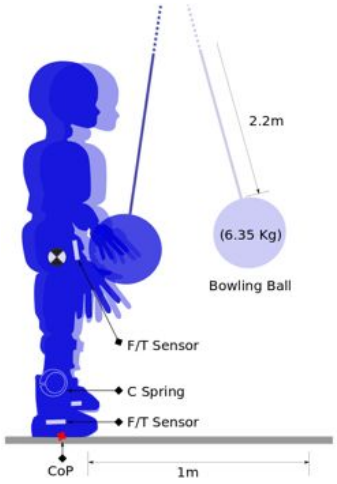

Fig. 6. A sketch of the first experimental scenario: : impact on the robot body.

system during the balancing task, which is determined, in the stiff case, only by the controller gains Kp, Kd (see previous section). Thus, in order to obtain a fair comparison, the gains of the balancing algorithm are adjusted in order to obtain the same equivalent stiffness at ankle joint (Fig. 5). Additionally, in order to simplify the analysis of our system, we activated the balancing controller only on the ankle forward/backward motion (one single degree of freedom), and turned off the body attitude controller [5] which is normally used to minimize for the spin angular momentum with the torso rotation. For each experiment, the impact force, the COP, the desired and the estimated COM position are recorded. The period of the control loop is one millisecond.

A. *Impact on the robot body*

In this experiment the robot, which is normally balancing on a static flat surface, is directly hit by a weight at the height of the COM, in the lower part of the torso. The weight is constituted by a standard bowling ball (6.35Kg), attached to the ceiling with a rope, about 2.20m long. The ball is released from a distance of 1.0m from the robot. A force sensor has been also placed at the point of impact, in order to obtain a direct measurement of the impact force. Fig. 6 illustrates the experimental setup previously described. After hitting the robot ten times releasing the ball always from the same distance with compliant and stiff ankles, Fig. 7 and Fig. 8 are obtained displaying mean and standard deviation values of the impact force, center of pressure, robot's COM and commanded COM for all trials with two different time scales (first 0.1 and 2 seconds respectively). The high repeatability of the experiment can be appreciated as well as the expected backwards motion of the center of pressure after the impact which happens much faster than the COM motion. At the macro time scale the controller exhibits a 60ms delay from the impact instant in both stiff and compliant cases, while the computed center of pressure presents a smoother behaviour in the compliant case right after the impact.

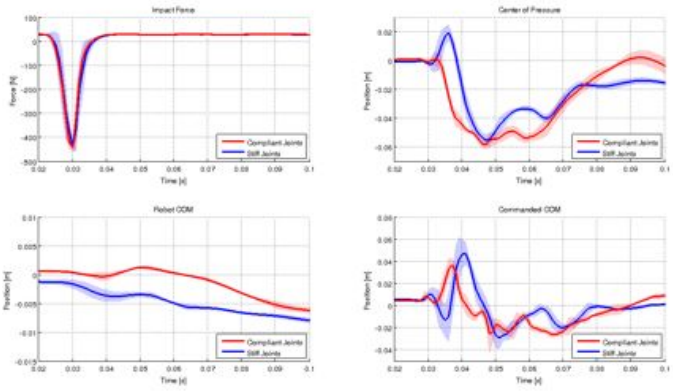

Fig. 7. The system response in the first 0.1 seconds after the impact (impact on the body).

B. *Impact on the platform*

Since appart from the CoP behaviour, no significant difference in the overall system behaviour is noticed between having compliance at the ankle level or not, a different experimental setup is used. This time the robot is balancing on top of a wheeled platform, which is hit by the weight in the same manner as in the former experiment. The force sensor is now located on the mobile platform, in order to measure the impact force. This is illustrated in Fig. 9.

Once more ten trials are done with both stiff and compliant ankles with high repeatability and small variance as can be seen in Fig. 10 and Fig. 12. When hitting the robot's COM, the linear momentum is instantaneosuly transmitted to the top part of the robot, which is not compliant like the ankle, probably masking up a more significat effect of the springs. For this reason, in this new setup the system is perturbed first at the ankle level by a quick backward motion of the supporting mobile platform. In this way, the linear momentum passes directly through the ankles and once more a filtering effect on the center of pressure can be observed also indicating a slower

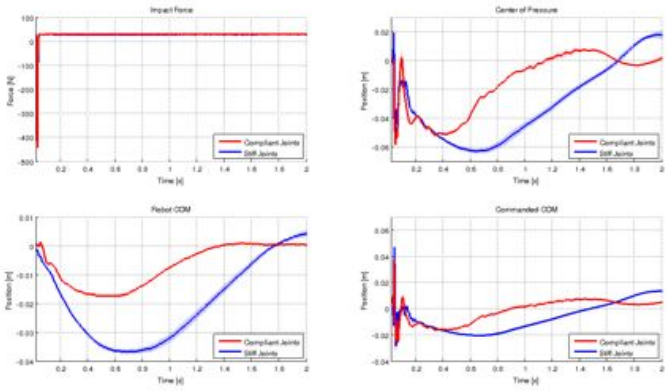

Fig. 8. The system response in the first 2 seconds after the impact (impact on the body).

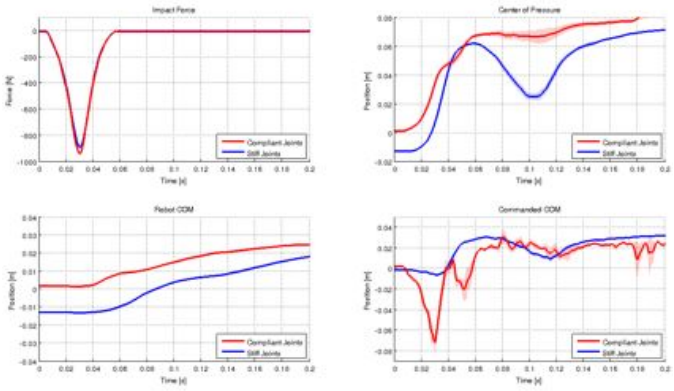

Fig. 10. The system response in the first 0.2 seconds after the impact (impact on the platform).

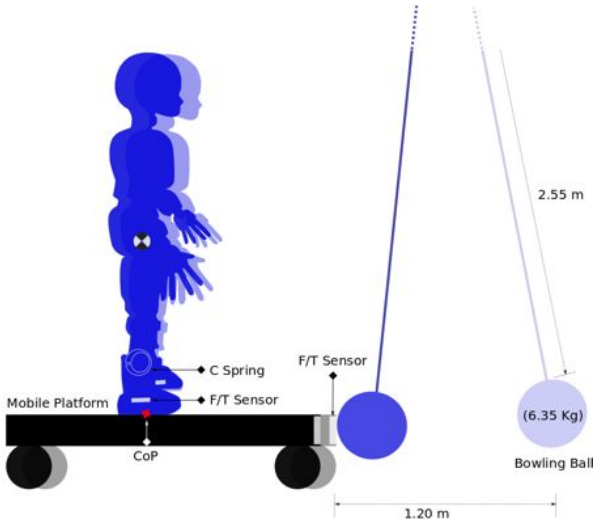

Fig. 9. A sketch of the second experimental scenario: impact on the platform.

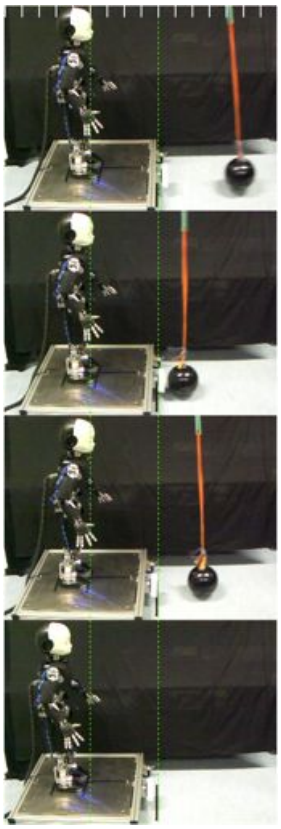

Fig. 11. A sequence of pictures showing the system balancing reaction after an impact on the support platform.

acceleration of the robot's center of mass. The effect is more noticeable at both micro and macro time scales.

V. Conclusions

In this paper we have shown the benefits of series elastic actuators in balancing tasks. The assumptions of the paper were to apply the very same perturbation on a standing robot, first equipped with series elastic actuators, then equipped with the same actuators but with the elastic transmission replaced with a rigid one. In order to perform a significant comparison experimental conditions were controlled in several ways. On one hand, perturbations were repeated several times, averaged over trials and standard deviations maintained relatively low for sake of repetitiveness. On the other hand, performances of the balance controller were made similar as much as possible. At the low level, actuators were controlled with a simple position controller whose gains were kept constant for both the rigid and elastic condition. At the high level, the center of pressure was controlled with a simple feedback strategy whose proportional gain was adapted to maintain constant the overall system stiffness, compensating for the transmission elasticity. Thanks to these conditions, the observed differences can be explained only with the different proportions between the active and passive stiffness. Results show shorter settling times in the case of series elastic actuators. Considering the experimental conditions, these results can be explained by the low pass filter effect of the series elastic actuators on the zero moment point dynamics.

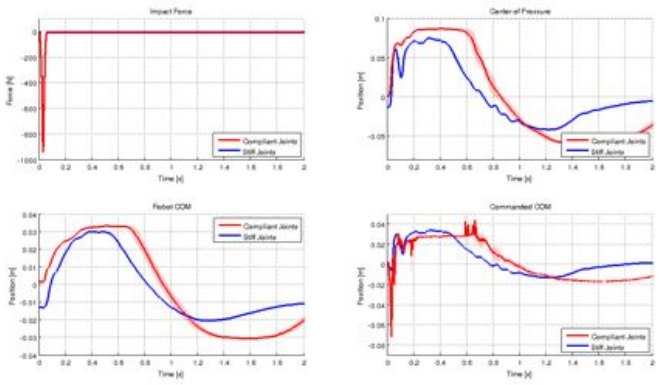

Fig. 12. The system response in the first 2 seconds after the impact (impact on the platform.

REFERENCES

[1] S. H. Hyon and G. Cheng, "Gravity compensation and full-body balancing for humanoid robots," in *IEEE-RAS International Conference on Humanoid Robots*, December 2006, pp. 214–221.

[2] B. Stephens and C. Atkeson, "Dynamic balance force control for compliant humanoid robots," in *IEEE/RSJ International Conference on Intelligent Robots and Systems*. IEEE, 2010, pp. 1248–1255.

[3] C. Ott, C. Baumgartner, J. Mayr, M. Fuchs, R. Burger, D. Lee, O. Eiberger, A. Albu-Schaffer, M. Grebenstein, and G. Hirzinger, "Development of a biped robot with torque controlled joints," in *10th IEEE-RAS International Conference on Humanoid Robots*, 2010, pp. 167–173.

[4] C. Ott, M. Roa, and G. Hirzinger, "Posture and balance control for biped robots based on contact force optimization," in *11th IEEE-RAS International Conference on Humanoid Robots (Humanoids)*, Bled, Slovenia, 2011, pp. 26–33.

[5] Z. Li, B. Vanderborght, N. G. Tsagarakis, L. Colasanto, and D. G. Caldwell, "Stabilization for the Compliant Humanoid Robot COMAN Exploiting Intrinsic and Controlled Compliance," in *IEEE International Conference on Robotics and Automation*, Minnesota, USA, May 2012.

[6] M. Hirose and K. Ogawa, "Honda humanoid robots development," *Philosophical Transactions of the Royal Society*, vol. 365, no. 1850, pp. 11–19, 2007.

[7] I. Park, J. Kim, J. Lee, and J. Oh, "Mechanical design of the humanoid robot platform HUBO," *Advanced Robotics*, vol. 21, no. 11, pp. 1305–1322, 2007.

[8] K. Kaneko, F. Kanehiro, M. Morisawa, K. Miura, S. Nakaoka, and S. Kajita, "Cybernetic human HRP-4C," in *Proc. IEEE/RAS Int. Conf. on Humanoid Robots (HUMANOIDS)*, 7-10 2009, pp. 7–14.

[9] T. Ishida, Y. Kuroki, and J. Yamaguchi, "Mechanical system of a small biped entertainment robot," in *Proc. IEEE/RSJ Int. Conf. on Intelligent Robots and Systems (IROS)*, October 2003, pp. 1129–1134.

[10] D. Gouaillier, V. Hugel, P. Blazevic, C. Kilner, J. Monceaux, P. Lafourcade, B. Marnier, J. Serre, and B. Maisonnier, "Mechatronic design of NAO humanoid," in *Proc. IEEE Int. Conf. on Robotics and Automation (ICRA)*, 2009, pp. 2124–2129.

[11] G. Pratt and M. Williamson, "Series elastic actuators," in *Proc. IEEE/RSJ Int. Conf. on Intelligent Robots and Systems (IROS)*, 1995, pp. 399–406.

[12] R. A. Brooks, C. Breazeal, M. Marjanovic, B. Scassellati, and M. Williamson, *The Cog project: Building a humanoid robot*. New York: Springer, 1999, p. 5287, lecture Notes in Artificial Intelligence 1562.

[13] J. Pratt and B. Kruppb, "Design of a bipedal walking robot." in *Proc. of SPIE*, vol. 6962, 2008, pp. 69 621F1–69 621F13.

[14] A. Edsinger-Gonzales and J. Weber, "Domo: a force sensing humanoid robot for manipulation research," *International Journal of Humanoid Robotics*, vol. 1, pp. 279–291, 2004.

[15] T. Lens, J. Kunz, O. Stryk, C. Trommer, and A. Karguth, "BioRob-arm: a quickly deployable and intrinsically safe, light-weight robot arm for service robotics applications," in *6th German Conference on Robotics (ROBOTIK)*. VDE, 2010.

[16] N. Tsagarakis, M. Laffranchi, B. Vanderborght, and D. Caldwell, "A compact soft actuator unit for small scale human friendly robots," in *Proc. IEEE Int. Conf. on Robotics and Automation (ICRA)*, may 2009, pp. 4356 –4362.

[17] N. Tsagarakis, Z. Li, J. Saglia, and D. Caldwell, "The design of the lower body of the compliant humanoid robot cCub," in *Proc. IEEE Int. Conf. on Robotics and Automation (ICRA)*, may 2011, pp. 2035 –2040.

[18] M. Grebenstein, A. Albu-Schaffer, T. Bahls, M. Chalon, O. Eiberger, W. Friedl, R. Gruber, S. Haddadin, U. Hagn, R. Haslinger, H. Hoppner, S. Jorg, M. Nickl, A. Nothhelfer, F. Petit, J. Reill, N. Seitz, T. Wimbock, S. Wolf, T. Wusthoff, and G. Hirzinger, "The DLR hand arm system," in *Proc. IEEE Int. Conf. on Robotics and Automation (ICRA)*, may 2011, pp. 3175 –3182.

[19] S. Wolf, O. Eiberger, and G. Hirzinger, "The DLR FSJ: Energy based design of a variable stiffness joint," in *Proc. IEEE Int. Conf. on Robotics and Automation (ICRA)*, may 2011, pp. 5082 –5089.

[20] C. A. Ihrke, A. H. Parsons, J. S. Mehling, and B. K. Griffith, "Planar torsion spring," U.S. Patent 2010/0 145 510 A1, Jun, 2010.

[21] S. P. Timoshenko and J. Goodier, *Theory of Elasticity*. McGraw-Hill, 1970.

[22] A. Parmiggiani, M. Maggiali, L. Natale, F. Nori, A. Schmitz, N. Tsagarakis, J. S. Viktor, F. Becchi, G. Sandini, and G. Metta, "The design of the iCub humanoid robot," *International Journal of Humanoid Robotics*, 2012, accepted for publication.